Chapter 4

A Hydrous Manganese Oxide Doped Gel Probe Sampler for Measuring *In Situ* Reductive Dissolution Rates: II. Field Deployment

Abstract

In situ rates of reductive dissolution in submerged shoreline sediments at Lake Tegel (Berlin, Germany) were measured with a novel hydrous manganese (Mn) oxide-doped gel probe sampler in concert with equilibrium gel probe and sequential extraction measurements. Rates were low in the top 8 cm, then showed a peak from 8 cm to 14 cm, with a maximum at 12 cm depth. This rate corresponded with a peak in dissolved porewater iron (Fe) at 11 cm depth. Below 14 cm, the reductive dissolution rate reached an intermediate steady value. Lower rates at depth corresponded with increases in operationally defined fractions of carbonate-bound and organic- and sulfide-bound Mn and Fe as detected by sequential extraction. Observed rates of reductive dissolution, which reflect a capacity for Mn reduction rather than actual rates under ambient conditions, appear to correlate with porewater chemistry and sequential extraction fractions as expected in early sediment diagenesis, and are consistent with previous measurements of *in situ* reductive dissolution rates. Significant downward advection in

this bank filtration setting depletes the Mn and Fe oxides in the sediments and enhances the transport of dissolved Fe and Mn into the infiltrating water.

Introduction

Biogeochemical processes in lacustrine and riverine sedimentary environments can affect the quality of the neighboring groundwater (von Gunten et al. 1994). During early sediment diagenesis, microbial reactions couple the decomposition of organic matter to terminal electron accepting processes (TEAPs), typically yielding a vertical sequence progressing from high to low energy yield TEAPs with increasing sediment depth (Berner 1980). Among these TEAPs, reductive dissolution of manganese (Mn) and iron (Fe) oxides, via microbially or chemically mediated reduction (Sunda et al. 1983, Burdige and Nealson 1986, Myers and Nealson 1988a, Waite et al. 1988), releases previously bound trace elements to the sediment porewater (Murray 1974, Davranche and Bollinger 2000, Monbet et al. 2008). Nearby groundwater pumping, as in bank filtration, can sustain a flux of organic matter from overlying water into sediments, which drives TEAPs (Wellsbury et al. 1996) and transports both their by-products and released trace elements into the groundwater (von Gunten et al. 1994).

In situ rates of Mn reductive dissolution have been previously approximated with steady-state diagenetic equations coupled to expressions describing solid phase Mn with depth (Robbins and Callender 1975, Burdige and Gieskes 1983, Sundby and Silverberg 1985). The assumed Gaussian shape of the reductive dissolution rate profile in diagenetic models has never been verified with field measurements, due to the lack of an appropriate

high-resolution, *in situ* measurement technique. Otherwise, environmental Mn reductive dissolution rates have been measured in sediment incubations from sediment cores (Canfield et al. 1993) and in an *in situ* bell jar (Balzer 1982), all of whose conditions inevitably differ from or disturb the actual setting. Building on the qualitative *in situ* Mn oxide redox indicator probe developed by Edenborn and Brickett (Edenborn and Brickett 2002, Edenborn et al. 2002) and high-resolution gel-based porewater samplers (Fones et al. 1998, Campbell et al. 2008a), an Mn oxide-doped gel probe has been developed for the quantification of *in situ* reduction rates (Farnsworth and Hering 2010).

Lake Tegel is a small eutrophic lake in northwest Berlin, Germany (Schauser and Chorus 2007), used for recreation and bank filtration for municipal water supply. Wastewater effluent (after secondary treatment) is released into the upstream tributaries of Lake Tegel. Because phosphorus (P) is the limiting nutrient, its release from or retention within the lake sediments affects the water quality of the lake (Schauser et al. 2006). The water extracted from bank filtration wells requires treatment for only Fe and Mn removal currently, but algal blooms in the lake could induce break-through of organic metabolites that would require additional drinking water treatment (Massmann et al. 2007).

The purpose of this study is to evaluate the *in situ* reductive dissolution rates in shoreline sediment at Lake Tegel using a novel Mn oxide-doped gel probe sampler in concert with standard sequential extraction and equilibrium gel probe techniques. Our results will provide new insight into rates of redox processes in an environment that is relevant for both drinking water and groundwater quality in this highly-managed setting.

Materials and Methods

Site description

Lake Tegel is a small lake (mean depth 7.6 m, surface area 3.06 km^2, residence time 77 d) in northwest Berlin, Germany (Figure 4.1). The flow of the Havel River, its southwestern tributary, mostly bypasses the lake, but some local mixing occurs as the lake discharges via this river (ca. 3.5 m^3 s^{-1}) (Schauser and Chorus 2007). Most of the lake is underlain by fine-grained, organic-rich sediments with low hydraulic conductivity (lacustrine sapropel), because of which most of the infiltrating water for bank filtration travels through permeable sand at the lake margins, where water depth is < 2 m (Massmann et al. 2007). All sampling conducted in this study occurred in sands along the eastern bank of Lake Tegel.

Reagents

All chemicals used were reagent grade and used without further purification. All water used was 18 MΩ-cm deionized water (Millipore). Solutions were stored in plastic containers that had been acid-washed in 5% hydrochloric acid. All nitric acid solutions were made with trace-metal-grade HNO_3 (Merck, Suprapur, 65%). All hydroxylamine solutions were made with trace-metal-grade hydroxylamine (Fluka).

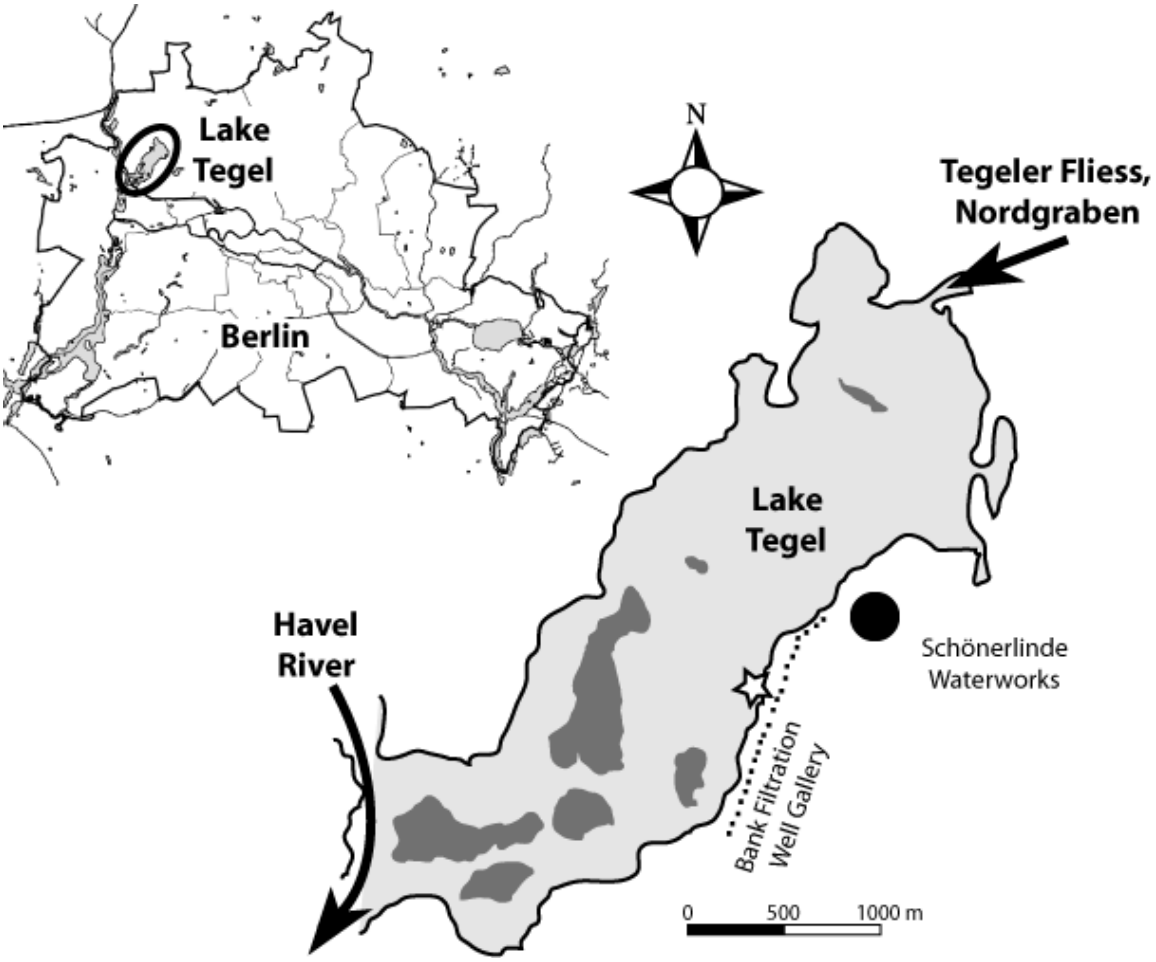

Figure 4.1. Location of Lake Tegel within Berlin city limits (upper left) and location of sampling site (star) within the lake (right; shaded regions indicate islands). Arrows indicate in- and outflows to the lake. Scale bar applies to right figure only.

Gel probe deployment

A complete description of HMO synthesis, clear and HMO-doped gel synthesis, re-equilibration, and analytical methods is provided in Part I (Farnsworth and Hering 2010). Two gel probes 35 cm long (Campbell et al. 2008b) were loaded with clear and HMO-doped gels, respectively. The gel slabs were secured with a 0.45 μm nitrocellulose membrane filter (Whatman, Protran) and held in place with a plastic face plate. The probes were placed in separate aluminum-coated O_2-impermeable polyethylene foil bags filled with deoxygenated water, bubbled with compressed N_2 gas for ≥ 24 h prior to

deployment to deoxygenate the water inside the gels, emptied of water, and welded shut for transport to the field, following Roberts et al. (2010).

The two gel probes were deployed back-to-back 3.75 m from the shore of Lake Tegel in July 2008. The foil bags were cut open on site, and the probes were inserted vertically into the sediments perpendicular to the shoreline, with several gels above the sediment-water interface (water depth 18 cm). The sandy sediments were soft up to 10 cm depth, below which they were hard; gel probes had to be hammered to the final depth of 25 cm. Wind-induced waves approximately 5 cm in height constantly propagated perpendicular to the shoreline, although no evidence of wave-driven sediment movement (e.g., ripples) was observed. Conditions during deployment were overcast, with intermittent light rain, and an average lake water temperature of 21°C (air temperature 18°C). The gel probes were allowed to interact with the sediment porewater for 48 h undisturbed before being extracted from the sediment. The gels were immediately removed from the probes and placed in individual, preweighed 2 ml tubes (Eppendorf), which were stored in ice during transport to the lab.

Upon arrival, the tubes (with gels) were weighed, and 1.25 ml 0.5% hydroxylamine HCl or 2% HNO_3 were added to the HMO-doped and clear gels, respectively. A minimum of 24 h later, these solutions were diluted for ICP-MS (Agilent 7500cx) analysis. The concentrations of Mn (or other solutes) from the gel solution was calculated as described previously (Campbell et al. 2008a).

Gel analysis

The calculation of the apparent rate coefficient for HMO reductive dissolution from HMO-doped gels is complicated by the need to account for the diffusion of dissolved Mn

out of the HMO-doped gel. A one-dimensional partial differential equation describing the dissolved Mn concentration within a gel (i.e., mol Mn per gel porewater volume) over the time of deployment was developed with Mn(II) assumed to be the only significant dissolved Mn species (Morgan 2000):

$$R = \frac{\partial}{\partial t} C_{Mn} = k' \cdot [HMO]_t - D \cdot \frac{\partial^2}{\partial x^2} [Mn(II)] \; . \qquad (4\text{-}1)$$

Here, the rate of change in Mn concentration in a gel (R, μmol ml^{-1} h^{-1}) is expressed as the difference between the rate of Mn(II) production inside the gel (i.e., reductive dissolution of HMO) and the rate of diffusion out of the gel (coefficient D, cm^2 h^{-1}). The chemical kinetics are represented as pseudo-first-order, with units of h^{-1} for k′, the apparent rate coefficient. The porewater outside a gel is considered to be an infinite sink for Mn(II), with a maximum concentration of C_{pw}, the porewater concentration measured by the clear gel at the same depth. [Mn(II)] is 0 within the gel initially, and [HMO] is initially the mean total Mn recovered from a single non-deployed gel (Mn_T), determined using 10–15 gels per batch of HMO-doped gels.

The gels give a measurement of the average rate of Mn loss over the time of probe deployment (R_{meas}): the total Mn (dissolved and solid) recovered from the gels after deployment can be subtracted from Mn_T and divided by the total time of deployment (48 h) (see Figure B.1). Iterating on k′ until the calculated R (R_{model}) is equivalent to R_{meas} gives the k′ for that gel.

A software file (see Appendix B) was developed for MATLAB to solve for k′ efficiently over an entire gel probe. Equation (4-1) was converted to the finite difference form below (equation (4-2)), which approximates the diffusion term via the central

difference theorem. The thickness of each gel (2 mm) was split into 5 equal "cells" (x-axis) for this approximation.

$$C_t^x = C_{t-1}^x + \delta t \cdot \left(k' \cdot HMO_{t-1}^x + \frac{D}{\delta x^2} \cdot \left(C_{t-1}^{x-1} - 2 \cdot C_{t-1}^x + C_{t-1}^{x+1} \right) \right) \quad (4\text{-}2)$$

$$HMO_t^x = HMO_{t-1}^x - \delta t \cdot \left(k' \cdot HMO_{t-1}^x \right) \quad (4\text{-}3)$$

$$R_{model} = \frac{Mn_T - \Sigma HMO_{48h}^x - \Sigma C_{48h}^x}{48\ h} \quad (4\text{-}4)$$

In the software code, C represents Mn(II) only, whereas HMO represents Mn(III,IV) solids, again as mol Mn per porewater volume of the gel (further description of parameters is given within code in Appendix B). In the calculation of R_{model} (equation (4-4)), HMO and C are summed over all 5 cells. The k′ for which R_{meas} - R_{model} is approximately 0 is approached with the secant method, until k'_{i+1} - k'_i = ± 0.05% k'_{i+1} or numerical precision of 3 significant digits for k′. The bounds of the 95% confidence interval for Mn_T are used to calculate error (accuracy) bounds for k′. Area-normalized rates were calculated by dividing R (mol l^{-1} h^{-1}) by the oxide surface area (m^2 g^{-1}), formula weight (g mol^{-1}), and concentration of Mn oxide per volume of porewater in the gel (mol l^{-1}).

Core processing and analysis

Two sediment cores were collected adjacent to the gel probes at the time of deployment, using 32 cm polycarbonate tubes with an internal diameter of 4.8 cm. One core was sliced immediately into 5 cm sections and stored in separate glass jars for porosity and particle-size measurements. The second core was transported on ice to the laboratory, where it was frozen until sequential extraction.

Physical parameters of sediment

Sediment sections from the first core were dried in an oven at 150°C overnight and sieved through a 500 μm sieve to remove large organic debris. Particle size and porosity measurements are detailed in Appendix B (Table B.1 and following). Hydraulic conductivity (K, expressed in cm s^{-1}) was calculated by solving

$$K = k_p \cdot \left(\frac{\rho \cdot g}{\mu} \right) \tag{4-5}$$

where k_p is intrinsic permeability (cm^2), ρ is the density of water (g cm^{-3}), g is the gravitational constant (980 cm s^{-2}), and μ is viscosity (g cm^{-1} s^{-1}). Because our sediment was reasonably well-sorted sand, we can estimate k_p with an empirical relationship presented by Bear (1972):

$$k_p = 0.617 \times 10^{-11} \cdot d \tag{4-6}$$

where d is the mean diameter of sediment particles expressed in μm.

Sequential extraction

In the laboratory, the second core was handled under N_2 in a glovebox for subsequent solid-phase extractions. The core was cut into 3 cm sections, the sediment mixed to homogenize the samples, and 3 samples taken from each section as replicates. The sequential extraction method (Table 4.1) is based upon the Peltier et al. (2005) modification of the Tessier method. The use of 20% H_2O_2, rather than 3.2 M ammonium acetate in 20% HNO_3 (Peltier et al. 2005), in step 4b and the solid-solution ratios were adapted from Ngiam and Lim (2001). For each sample, 2–3 g of wet sediment were transferred into 50 ml centrifuge tubes, followed by the reagents for each step. After each extraction step was completed, the samples were centrifuged at 1900g for 12 min,

and the resulting supernatant was filtered through a 0.45 μm cellulose acetate filter and saved for analysis. Between each reaction step (except between 4a and b), samples were rinsed with 8 ml deionized water, which was saved after a second centrifugation. All steps prior to the organic and sulfide extraction were carried out under N_2 in a glovebox, except the heating portion of step 3, which was carried out in a fume hood with minimal infiltration of O_2 into the reaction vials.

Table 4.1. Experimental conditions for modified Peltier method sequential extraction

step	extractant	target
1	8 ml 1 M MgCl, 1 h	exchangeable
2	8 ml 1 M Na-acetate, pH 5, 5 h	carbonate
3	20 ml 0.04 M hydroxylamine HCl in 25% acetic acid, 6 h at 75 °C	reducible oxides
4a	5 ml 30% H_2O_2 and 3 ml 0.02 M HNO_3, pH 2, 2 h at 75 °C	organics, sulfides
4b	3 ml 30% H_2O_2, pH 2, 2 h at 75 °C	
5	12 ml aqua regia, 24 h then 2 h at 75 °C	residual (nonsilicate)

Samples were diluted with 2% HNO_3 and analyzed by ICP-MS. Element concentrations were converted to percentages of the total amount extracted from the sample, omitting the contributions from silicate-bound minerals not extracted in this method. Concentrations were normalized to the dry weight of the sample, as measured by drying sediment from each core section in an oven for 24 h at 140°C.

Results

The porewater concentrations in Lake Tegel near-shore sediments were low in all tested trace elements except Fe and Mn (Table B.2, Figure 4.2a). Subsequent results and discussion focus on these two redox-active elements. Dissolved Fe was 1–2 orders of magnitude higher in concentration than dissolved Mn throughout the profile. Dissolved

Mn was less than 1 μM in the overlying water (-10 to 0 cm depth) and below the sediment-water interface to a depth of approximately 12 cm, below which the concentration gradually approached 5 μM. Elevated Mn concentrations were observed in two isolated samples at 20 and 22 cm depth. Dissolved Fe, on the other hand, shows a distinct peak between 4 and 18 cm depth, with a maximum of 134 μM at 11 cm. Below the peak, the Fe concentration (15 μM) is still higher than the concentrations (< 1 μM) in the overlying water and in the sediment porewater between 0 and 4 cm depth.

The profile of rate coefficients with depth (Figure 4.2b) also exhibits a distinct maximum at 12 cm. The profile reflects almost no reduction in the overlying water or between 0–1 cm depth in the sediment. The rate coefficients then gradually increase from 0.002 to 0.006 h^{-1} between 1 and 8 cm in depth ("shallow" rate coefficient), at which point a broad peak is observed, extending from 8 to 14 cm depth. The maximum rate coefficient, 0.103 h^{-1}, is two orders of magnitude faster than that at shallower depths. Below 14 cm, the rate coefficient appears to fluctuate around a lower mean of 0.031 h^{-1} ("deep" rate coefficient). Below 22 cm, the rate coefficient decreases to 0.019 h^{-1} at 24 cm depth.

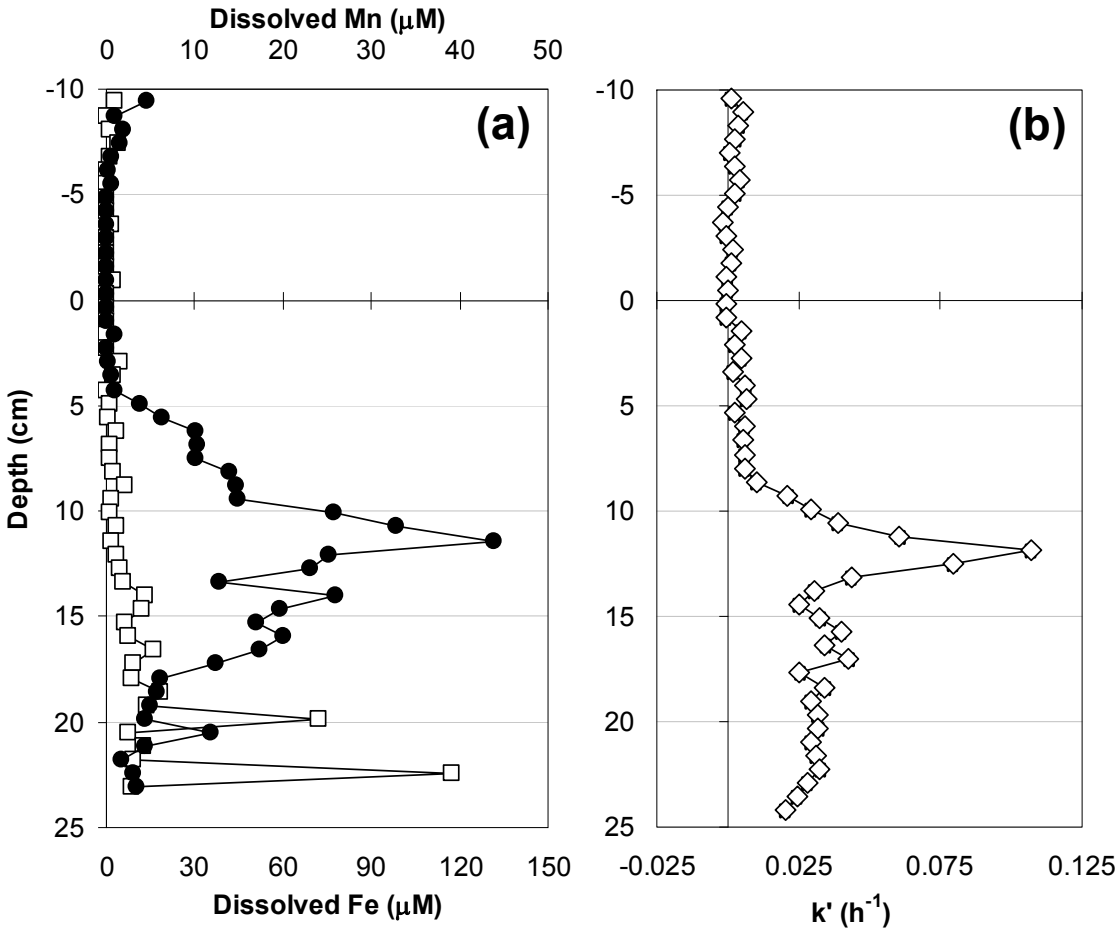

Figure 4.2. Porewater concentrations of dissolved Mn (□) and Fe (●)from clear gel probe (a), and apparent pseudo-first-order rate coefficient k′ (◇) from HMO-doped gel probe (b). Bars representing error bounds for k′ are sometimes smaller than the data markers. The probes were deployed back-to-back for 48 h in July 2008.

The sequential extraction method should recover all Fe and Mn in the sediment except for the silicate-bound fraction. Total recovered Mn ranged between 6 and 32 mg kg^{-1} over 25 cm depth (Figure 4.3). Total recovered Fe was much higher, ranging between 180 and 1100 mg kg^{-1} over the same depth. The highest amounts of both elements were recovered in the 7–10 cm section, with a decline in concentration as the depth increased, except in the 19–22 cm section.

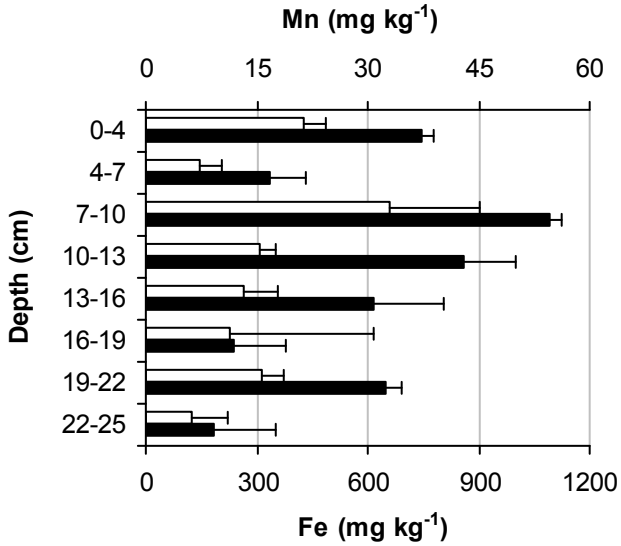

Figure 4.3. Total extracted Mn (white) and Fe (black) from sediment cores in sequential extraction. Bars are averages of 3 subsamples for each core section (standard deviation shown).

Individual, operationally defined fractions of Fe and Mn also varied with depth (Figure 4.4, Figure B.2). Manganese generally had high "exchangeable" fractions at all depths (11–55%), whereas Fe had essentially no "exchangeable" fraction (< 1%). "Carbonate-bound" Mn and Fe fractions were measured at depths greater than 16 cm, and were relatively small (4–16% Mn; < 2% Fe). "Reducible oxides" of Mn and Fe were highest at the surface-water interface, and decreased with depth. For both Fe and Mn, the fraction of "organic- and sulfide-bound" was low at the surface-water interface, increased to a maximum at 13–16 cm depth, and decreased again with depth. The "residual" fraction varied with depth, generally composing 24–78% of the total Fe and a lesser proportion of the total Mn (2–49%).

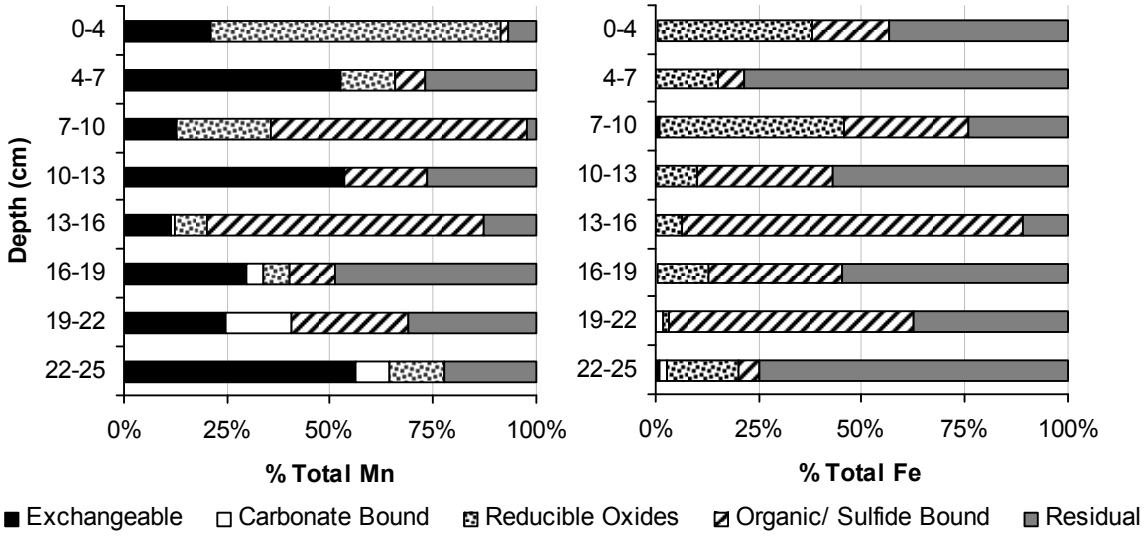

Figure 4.4. Manganese and iron concentrations measured in sediments, expressed as percentage of the total elemental concentration recovered in all 5 sequential extraction steps (given in Figure 4.3). The plotted bars are averages of 3 subsamples for each core section.

Porosity ranged from 0.41 to 0.55 (mean = 0.48) and generally increased with depth (Table B.1). Sediment was sandy, and mean particle size values were generally consistent with the trend in porosity, ranging from 215 to 332 μm (mean of all samples = 294 μm) and generally decreasing with depth, except for the deepest sample (Table B.1). Visual observations suggest that a minor peak in the particle size histograms of sediment samples from deeper core sections (Figure B.3) may result from decomposing organic matter, since varying amounts of fine, black particles were interspersed with coarse, brown sand. These black particles were more numerous in core sections that contained more large organic debris, which was partially decomposed. The temperature of the shallow groundwater sampled in this study was assumed to be equal to the measured lake water temperature, 21°C. Using this temperature, K was estimated to range from 3.90×10^{-2} to 6.71×10^{-2} cm s^{-1} (mean = 5.29×10^{-2} cm s^{-1}; Table B.2), which is similar to the range of a moderately permeable aquifer (Bear 1972).

Discussion

Trends with sediment depth

The variation of the measured reductive dissolution rate coefficients with sediment depth corresponds with indications of expected sediment diagenesis (Berner 1980). The low rates of reductive dissolution in the overlying waters and first cm of sediment likely indicate that microbial respiration is supported by more thermodynamically favorable TEAs (i.e., dissolved oxygen and/or nitrate, which are present in the overlying water at saturation (Massmann et al. 2006) and an average concentration of 280 μM (Ziegler 2001), respectively). As these TEAs are depleted in the upper sediments (i.e., 1–8 cm), dissolved Fe and Mn would then be produced by reductive dissolution. The low porewater Fe concentration above 4 cm could indicate that aerobic or anaerobic Fe oxidative precipitation occurs as the dissolved Fe produced deeper in the sediments diffuses upwards. However, low porewater Fe could also reflect downward advection in these sediments.

The peak in reductive dissolution observed with the HMO-doped gel sampler occurs at nearly the same depth as the peak in porewater Fe. Just above this, the highest amounts of sediment-bound Fe and Mn occur in the 7–10 cm section. The "reducible oxide" fraction of Mn is at a minimum at 10–13 cm, and the corresponding Fe fraction is similarly low between 10 and 16 cm depth. Active reductive dissolution of these solid fractions, as suggested by the facile reduction of introduced HMO, could explain these low fractions. Although sulfide fractions can be prematurely extracted with the "reducible oxide" fraction (Peltier et al. 2005), this artifact is less significant for Mn, because Mn is not appreciably associated with sulfide in freshwaters (Berner 1980).

"Organic- and sulfide-bound" Mn is therefore likely dominated by organic-bound Mn. In contrast, freshly formed amorphous Fe-sulfides are susceptible to premature extraction as "reducible oxides" (Peltier et al. 2005).

Decreasing porewater Fe concentrations below 12 cm indicate that dissolved Fe production is decreasing with depth, sequestration of dissolved Fe is faster than its production, or some combination thereof. The depth profile in HMO reduction (i.e., lower, relatively constant rates below 14 cm) suggests that the production of dissolved Fe may indeed decrease between 12 and 15 cm. More likely responsible for the bulk of the decreasing porewater Fe is greater dissolved Fe sequestration at depth. The appearance of "carbonate-bound" fractions below 16 cm and elevated "organic- and sulfide-bound" Fe fractions between 13 and 22 cm suggest carbonate and sulfide precipitation are prevalent at these depths. "Reducible oxide" fractions at these depths represent either more crystalline, refractory Fe and Mn oxides (Berner 1981, de Vitre et al. 1988, Burdige et al. 1992), or premature oxidation of sulfide-bound Fe (Peltier et al. 2005). Hence, the measured rates of reductive dissolution are consistent with observed sediment processes.

In situ *rates and reductants*

The range of reported Mn reductive dissolution rates is wide, and generally lower than the rates measured in these sediments (Table 4.2). Surface-area-normalized rates either measured or calculated from diagenetic models ranged from 5.4×10^{-11} mol m^{-2} h^{-1} in the equatorial Atlantic Ocean (Burdige and Gieskes 1983) to 1.9×10^{-4} mol m^{-2} h^{-1} in the Gulf of St. Lawrence (Sundby and Silverberg 1985). No clear trends with fresh or saline waters were obvious, nor were rates from diagenetic models significantly different from direct measurements. In contrast, the nutrient load in the water body seemed to be

significant; eutrophic water bodies generally had faster Mn oxide reduction rates in their sediments. The maximum rate from our study was among the faster rates in the literature, within the ranges measured in the Gulf of St. Lawrence (Sundby and Silverberg 1985) and the eastern Danish coast (Balzer 1982). The "shallow" and "deep" rates from our study were mid-range, similar in magnitude to that measured in Long Island Sound (Burdige and Gieskes 1983).

Table 4.2. Surface-area-normalized Mn reduction rates from field studies

Source	Location	Rate[a] (mol m^{-2} h^{-1})	Diagenetic Model	Eutrophic
[1]	equatorial Atlantic Ocean	5.4×10^{-11}	yes	no
	Chesapeake Bay	4.6×10^{-10}	yes	yes
[2]	AMD wetland[b]: shallow	8.4×10^{-8}	no	no
[3]	Lake Michigan	9.2×10^{-8}	yes	no
[2]	AMD wetland[b]: maximum	1.7×10^{-7}	no	no
[4]	North Sea: Skagerrak Basin	$3.2\text{-}16 \times 10^{-7}$	no	no
[1]	Long Island Sound	6.7×10^{-7}	yes	yes
This Study	Lake Tegel: shallow	9.4×10^{-7}	no	yes
	Lake Tegel: deep	7.3×10^{-6}	no	yes
	Lake Tegel: maximum	2.4×10^{-5}	no	yes
[5]	eastern Danish coast	$1.5\text{-}4.9 \times 10^{-5}$	no	yes
[6]	Gulf of St. Lawrence	$1.3\text{-}19 \times 10^{-5}$	yes	yes

[a] See Table B.3 for calculation details.
[b] Constructed wetland to treat acid mine drainage
Sources: 1 Burdige and Gieskes (1983); 2 Edenborn and Brickett (2002); 3 Robbins and Callender (1975); 4 Canfield et al. (1993); 5 Balzer (1982); 6 Sundby and Silverberg (1985)

Ideally, pseudo-first-order rate coefficients obtained in our study could be tied to experimentally derived rate coefficients in literature to help identify the possible *in situ* Mn oxide reductants. The pseudo-first-order rate coefficient (k′) should correspond to the laboratory-derived rate coefficient (k) for a given reductant (Red) as shown in Equation (4-7):

$$k' = k\,[Red] \quad (4\text{-}7)$$

where pseudo-first-order behavior is expected only for approximately constant Red concentrations. Laboratory reduction rate coefficients are available for a variety of reductants with Mn oxide in conditions similar to those at Lake Tegel (freshwater at pH ~ 8 (Massmann et al. 2006)) and are tabulated for probable environmentally relevant reductants (i.e., Fe(II), S(-II), *S. oneidensis* str. MR-1, and humic and fulvic acids) in Table 4.3. In addition, ascorbate, a strong chemical reductant for Mn oxide not anticipated to accumulate significantly in this setting, was added for comparison. Under the three distinct zones of the rate coefficient profile, shallow, maximum, and deep, the amount of Red required to generate the observed pseudo-first-order rate coefficient was calculated ($[Red]_{reqd}$).

These required reductant concentrations are uniformly lower than the measured or estimated concentrations of reductants in Lake Tegel sediments. For example, the rate coefficients for Fe(II) predict that approximately 1 μM Fe(II) could produce the observed maximum pseudo-first-order rate coefficient. However, the actual porewater Fe concentration of 134 μM suggests that the *in situ* rate should be ~ 100× faster. Discrepancies between $[Red]_{reqd}$ and the actual or estimated reductant concentrations are similarly 1–2 orders of magnitude for S(-II), *S. oneidensis* MR-1, and perhaps even humic and fulvic acid. Although preliminary work concluded that HMO-doped gels only capture 35% of microbial reduction due to the lack of direct contact between the cell wall and the Mn oxide, no incomplete measurement was observed for chemical species (Farnsworth and Hering 2010). If the measured pseudo-first-order rate coefficients are accurate, as suggested by the earlier comparison with literature *in situ* reduction rates

(Table 4.2) and preliminary work with Mn-doped gels (Farnsworth and Hering 2010), then the observed and required reductant concentrations suggest that the extrapolation from laboratory to field conditions is not valid for Lake Tegel. This could reflect a limitation of sediment microbial activity by organic carbon or a trace nutrient, as compared to laboratory media optimized for growth.

Table 4.3. Summary of literature values for Mn oxide reduction rate coefficients

Source	Red	log k [units^{-1} h^{-1}]	units	$[Red]_{reqd}$ shallow (-2.40)[a]	max (-0.99)[a]	deep (-1.51)[a]
[1]	Fe(II)	4.97	μM	0.043	1.1	0.34
[2]	Fe(II)	4.92	μM	0.048	1.2	0.37
[3]	Fe(II)	5.66	μM	0.009	0.2	0.07
	Obs rved		μM	30	134	15
[1]	S(-II)	3.66	μM	0.87	22.3	6.71
	Estimated[b]		μM			77
[4]	MR-1[c]	-12.0	cells l^{-1}	3.7×10^{9}	9.6×10^{10}	2.9×10^{10}
[2]	MR-1[c]	-11.8	cells l^{-1}	2.6×10^{9}	6.8×10^{10}	2.1×10^{10}
	Estimated[d]		cells l^{-1}	1×10^{13}	5×10^{12}	1×10^{12}
[5]	Humic Acid	-0.40	mg l^{-1}	.010	0.258	0.077
[6]	Fulvic Acid	-0.30	mg l^{-1}	0.008	0.206	0.062
[4]	Ascorbate	4.18	μM	0.267	6.9	2.07

[a] log (k′ [h^{-1}]) numbers in parentheses
[b] Estimated from maximum sulfate concentrations in Lake Tegel sediments (Schauser et al. 2006)
[c] *S. oneidensis* str. MR-1
[d] Estimated from depth profiles of total cell number in freshwater river mudbank sediment (Wellsbury et al. 1996)
Sources: 1 de Vitre et al. (1988); 2 Burdige et al. (1992); 3 Myers and Nealson (1988a); 4 Farnsworth and Hering (2010); 5 Sunda et al. (1983); 6 Waite et al. (1988)

It is, however, important to bear in mind that the introduction of the HMO-doped gel probe represents a perturbation of ambient conditions. In the case of Lake Tegel sediments, the microbial community is presented with a substrate that is relatively depleted in the ambient sediments. Although the microbial community at some depths may quickly commence Mn reduction, especially in zones of Fe reduction (Blakeney et al.

2000), the community in other zones must acclimate to the given substrate in a relatively short period of time (48 h). Thus the Mn reduction observed with the HMO-doped gel probe corresponds to a capacity for Mn reduction rather than an actual rate under ambient conditions.

Impact of field setting on rates

The sediments at the shoreline of Lake Tegel are not representative of the whole lake, although local homogeneity was observed on the scale of 5–10 m. Chemically, sediments in the lake basin were found to have 30× the Fe content of our shoreline sediments (30 mg kg^{-1} vs. > 1 mg kg^{-1}), as well as higher porewater dissolved Fe and Mn in the top 5 cm (Schauser et al. 2006). Physically, basin sediments are fine-grained lacustrine sapropel with lower hydraulic conductivity than the sandy shoreline sediment (Massmann et al. 2007), which is significant in light of the extensive groundwater pumping adjacent to Lake Tegel (~ 100 m inland; Figure 4.1): the majority of infiltrating water travels through the clogged permeable sands at the lake margins (Massmann et al. 2007). In fact, the lake margins are seasonally perched > 2 m below the sediment-water interface during the summer's low flows and high drinking water demand (Ziegler 2001). Hence, the shoreline setting is more relevant for solute behavior in infiltrating water.

Advection into the groundwater table, while not impacting the calculations of the *in situ* rate coefficients, certainly affects the chemistry of the sediments. The constant reaction of Fe and Mn oxides in the absence of significant input to the sediments leads to their exhaustion, especially in the case of less abundant Mn oxides (von Gunten and Zobrist 1993). In an experimental manipulation, the isolation of ocean basin sediments from particulate input resulted in the exhaustion of Mn oxides in ~ 100 d (Balzer 1982).

The relative lack of "reducible oxides" at and just above (10–16 cm depth) the peaks in dissolved Fe and reduction rate (12 cm) reflects reductive dissolution over a long time scale without comparable Fe and Mn oxide input. Subsequent transport through sediments and aquifer material prevents diffusion of reduced Fe and Mn to oxic regions, where it might be reoxidized. Reduced Mn and Fe thus travel along the bank infiltration flow path, as is typical in eutrophic bank filtration systems (von Gunten et al. 1994).

Acknowledgements

Sarah Griffis, supported by a Caltech Summer Undergraduate Research Fellowship, performed sequential extractions of sediments. Rich Wildman measured sediment particle size and assisted in the assessment of advection at Lake Tegel. We thank G. Massmann and T. Taute for useful site discussions and coordination with the Berlin Waterworks (Berliner Wasserbetriebe). We also thank J. Morgan and J. Adkins for helpful discussions about HMO-doped gel probe deployment and modeling, S. Hug and L. Roberts for assistance with the foil gel probe pouches, R. Saladin, M. Bonalumi, M. Kunz, and A. Müller for assistance with particle size analysis, and M. Huettel for helpful discussions regarding groundwater flow. We gratefully acknowledge funding from Eawag and NSF EAR-0525387, as well as support from an NSF Graduate Research Fellowship.